Russian Journal of Biomechanics, vol.6,N4: 52-62, 2002.

PULSE WAVE REFLECTIONS IN ASYMMETRICALLY BRANCHING ARTERIAL NETWORKS

M.Ye.Bondarenko, N.N.Kizilova

Department of Theoretical Mechanics, Kharkov National University, 4, Svobody Sq., Kharkov, Ukraine

Abstract: Wave propagation and reflection in the model of asymmetrically branching tree of elastic cylindrical tubes filled with nonviscous fluid is considered when applied to pulse wave reflection in arterial networks. Influence of the geometrical and mechanical properties of the network and vessel wall on the pulse wave propagation and spectral properties of the total admittance of the network are investigated.

It was found out that the admittance of the tree has a set of resonant harmonics. Any changes in parameters of microcirculatory bed cause noticeable alterations of the amplitudes of resonant harmonics and negligibly small alterations of other harmonics. The set of resonant harmonics is independent of some variations in the tree geometry. These results substantiate a possibility of the pulse diagnosis of inner organs state by observation the amplitudes of the resonant harmonics only without preliminary knowledge of individual structure of real vascular bed of an inner organ.

Key words: pulse wave reflections, cardiovascular system, branching transport networks, pulse diagnosis.

Introduction

Pulsatile blood flow in cardiovascular system is produced by heart contraction and determined by a number of factors [1]. The hydrodynamic analysis of the flow must take into consideration certain properties such as arterial network geometry, arterial branching and vascular wall properties, blood rheology. The elasticity of the arterial walls is responsible for transforming the oscillatory cardiac outflow into a relatively steady blood flow in peripheral

vessels. Any inhomogeneity in both the geometrical and mechanical properties of vessels produces backward pulse wave.

Pressure and flow waves change in shape and size as they travel through the network owing to the superposition of the forward and backward waves. The diameter of elastic vessels varies throughout the cardiac cycle. The diameter variations can be palpated on some superficial arteries with (the deep pulse) or without (the superficial pulse) an outer compression. The skill of inner organs and regulatory systems evaluation by radial artery examination forms the basis of the pulse diagnosis in oriental medicine. The recent investigations make it possible to offer a new diagnostic method that is based on the concept of the so-called resonant frequencies [2]. Numerous experimental investigations and clinical observations revealed the existence of the unique set of resonant frequencies in Fourier spectrum of pulse of some inner organs (kidneys [3], liver [4], spleen [5] and gall bladder [6]). The corresponding amplitudes depend on the organ state (normal or pathological) and show the organ state in excess-deficiency terms inherent in the oriental medicine. The pulse wave parameters can be estimated on any peripheral artery with a cuff manometer only at the absence of preliminary special compressions of the artery. The nature of the resonant frequencies is still unknown whereas the method itself has been used in clinics [3-6]. The experimental measurements and theoretical investigations with application of electrical analogous models show that the main resonant frequency is connected with the length of the largest (supplying) artery of the organ network [7].

The main properties of blood flow can be described on the basis of steady flow in a rigid cylindrical tube (Poiseuille's flow). The features of the pulsatile flow, the influence of arterial wall properties on the motion were investigated on the basis of Windkessel model (or Frank's elastic chamber) [1]. This model even in the modified form did not take into account the arterial network structure and can not explain pulse wave propagation and reflection features in different inner organ networks and in aorta. A general model based on the laws of classical mechanics was introduced by L.Euler (1755) and was extended in a series of papers by I.S.Gromeka (1883),

Witzig (1914), J.R.Womersley (1957). This model deals with a single cylindrical elastic tube in which the blood motion is described by differential equations based on the conservation laws of mechanics. A circulatory bed can be represented by a branching network of such tubes with different lengths and diameters. The value of input or effective admittance of the vascular network ($Y_{in} = Q/P$, P – pressure, Q – the volumetric rate of flow in the longitudinal direction in the initial section of the supplying artery) can be obtained as a function of the network geometry and wall properties. Rather complete results were obtained for some dichotomous branching trees [8]. More realistic results have been obtained on the basis of the same theoretical model with precise morphometric data of coronary network construction [9]. In the present work the influence of geometrical and mechanical properties of arterial network on pulse wave propagation and spectral properties of the vascular bed admittance are investigated.

Single tube with terminal element.

One-dimensional motion of homogeneous nonviscous incompressible fluid in thin-walled elastic cylinder tube is considered. The tube is terminated by a Windkessel element (terminus) with the input admittance $Y_t = Y_1 + iY_2$, where $Y_{1,2}$ – resistive and capacitive parts of the admittance, respectively. The fluid viscosity was neglected because of practically flat velocity profiles in the cross-sections of the arteries [1]. The pulse wave velocity reaches at last $c = 5$ m/c in elastic arteries, while velocity length $\lambda >> d$, where d – vessel diameter. Thus, the profiles can be considered to remain flat during a cardiac cycle. The mass and impulse conservation laws in quasi-one-dimensional form are expressed by the following equations [10]:

$$\frac{\partial A}{\partial t} + \frac{\partial}{\partial x}(AU) = 0 \qquad (1)$$

$$\frac{\partial U}{\partial t} + U\frac{\partial U}{\partial x} = -\frac{1}{\rho}\frac{\partial P}{\partial x} \qquad (2)$$

$$A = A(p)$$

where A denotes cross section of the tube, $U(t,x) = Q/A$ – average cross-sectional velocity, ρ – density of the fluid. The boundary conditions are:

$$P(t,0) = P_0(t),\ U(t,0) = P_0(t)Y' \tag{3}$$

$$P(t,L) = P_t(t,0),\ Q(t,L) = Q_t(t,0) = Y_t P(t,L) \tag{4}$$

where P_t, Q_t – pressure and volumetric flow rates in the terminus, Y' – input admittance of the whole system $Y + Y_t$, $Y = A/(\rho c)$ – characteristic admittance of the tube, L – length of the tube. Here relations (4) represent the conditions of pressure and flow continuity at the tube and terminus joint. From (1)–(2) the wave equation for the pressure can be obtained:

$$\frac{\partial^2 P}{\partial t^2} = c^2 \frac{\partial^2 P}{\partial x^2}$$

where $c = \left(\frac{A}{\rho} \frac{dP}{dA} \right)^{1/2}$ – velocity of the both forward and backward pulse waves.

The backward wave appears at the terminus and superimposes the forward wave. Wave reflections modify the flow through a tube by altering the pressure distribution within the vessel and, therefore, modifying the effective admittance of the system. While the characteristic admittance Y depends on the vessel properties only, the effective admittance Y' depends on relationship between pressure and flow, thus, is affected by wave reflections [9].

For homogeneous thin-walled elastic tube $c = \sqrt{Eh/\rho d}$, where E – Young's modulus for wall material, h – wall thickness. The solution of (1)–(3) may be obtained as superposition of the forward and backward waves:

$$P(t,x) = P_f e^{i\omega t}(e^{-i\omega x/c} + e^{i\omega(x-2L)/c}) \tag{5}$$

$$Q(t,x) = YP_f e^{i\omega t}(e^{-i\omega x/c} - e^{i\omega(x-2L)/c}) \tag{6}$$

where $Y = A\sqrt{d/(\rho Eh)}$ – characteristic impedance of the tube, Γ – reflection coefficient at the terminus, $\omega = 2\pi f$ – frequency of the wave. From (3)–(6) we finally receive the relation for effective admittance of the system:

$$Y' = Y\frac{1-\Gamma\exp(z)}{1+\Gamma\exp(z)} \qquad (7)$$

where $\Gamma = (Y - Y_t)/(Y + Y_t)$, $z = -2i\omega L/c$. As a result, the system $Y + Y_t$ can be represented as a single tube with complex admittance Y'.

Asymmetric dichotomous branching arterial tree

A branching system consisted of thin-walled elastic tubes is considered here (Fig.1–2). The branching order numeration of a tube is introduced by the rules:

1) the supplying artery has the order $i = 0$;

2) two tubes with the orders i_1 and i_2 after their connection form a tube with the order

$$i = \begin{cases} i_1, & i_1 = i_2 \\ \max\{i_1, i_2\}, & i_1 \neq i_2 \end{cases}$$

Each tube with the largest branching order $i = n$ terminates by the Windkessel element Y_t. The influence of branching angles on wave reflections will be considered negligibly small [1]. Thus, the pulse wave reflection in the system is fully defined by the set $J = \{d_j, L_j, h_j, E_j\}_{j=1}^{N}$ of predetermined mechanical and geometrical properties of separate vessels of different branching orders $j = 1 \div n$, where N – total number of vessels in the system. Generally, the full set J has to be introduced using the morphometric data.

Vascular beds of different organs exhibit certain regularities in geometry [11]. These regularities may be represented as the ratio between the average values of diameters and/or lengths of the consecutive vessels $L_j / L_{j+1} = b_L = \text{const}$, $d_j / d_{j+1} = b_d = \text{const}$ or as a relation between the diameters $d_j^{0,1,2}$ of parent and daughter vessels in bifurcation as follows:

$$\left(d_j^0\right)^\gamma = \left(d_j^1\right)^\gamma + \left(d_j^2\right)^\gamma \qquad (8)$$

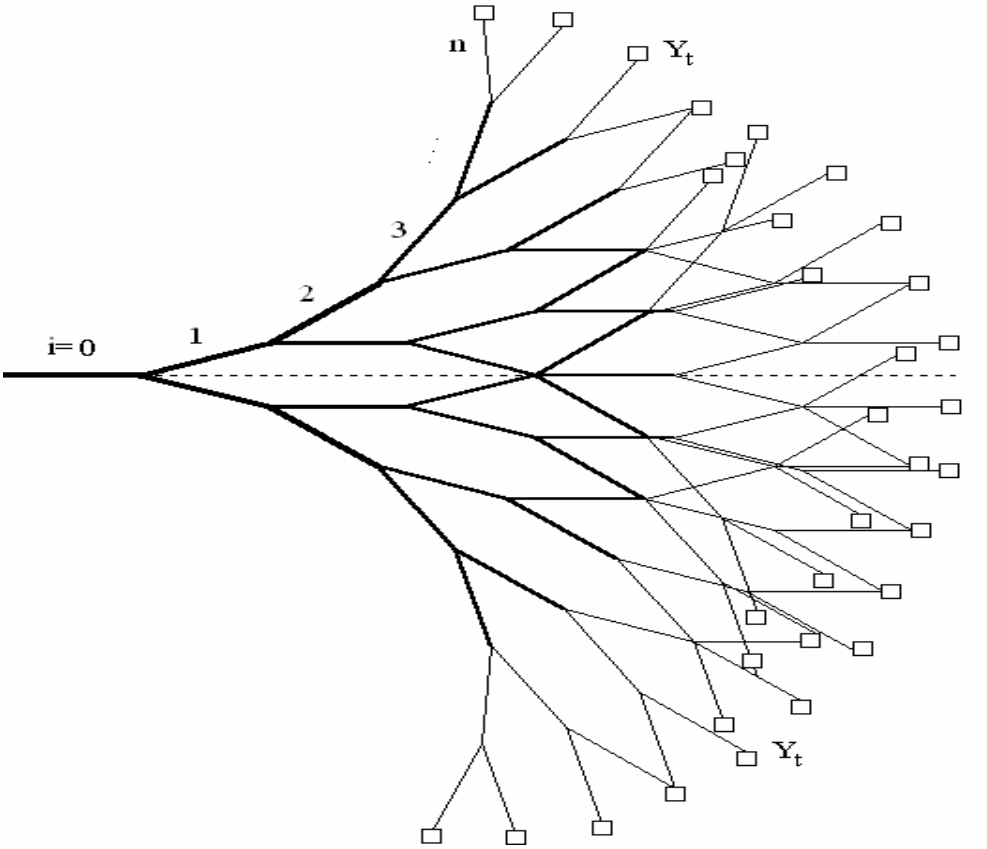

Fig.1. Symmetrical dichotomous branching arterial tree with $\xi, \zeta, b_L = 1,\ b_R = 0.9$.

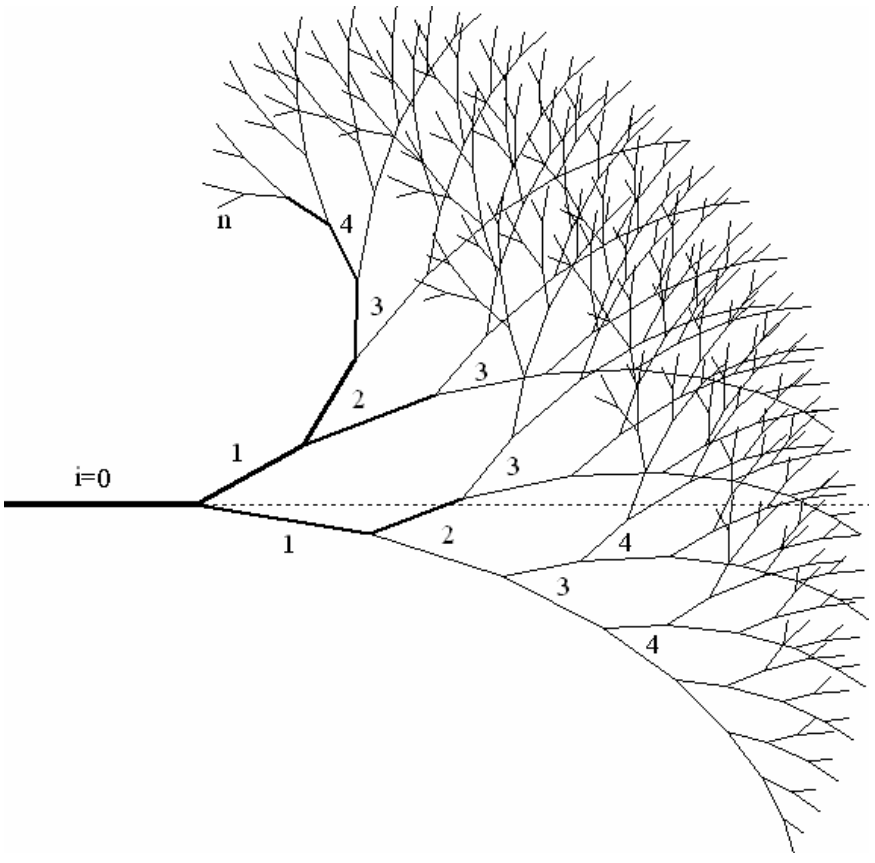

Fig.2. Asymmetrical dichotomous branching arterial tree with $\xi = \zeta = 0.7\ b_L = 1,\ b_R = 0.9$.

The majority of vascular networks in animal and plant tissues have $\gamma = 2.33 - 3.01$ [12]. The networks exhibit self-similarity and optimal transport properties. Their geometry promotes minimising of the total cost of fluid delivering, network construction and maintenance. For the self-similar optimal transport systems the following relations may be introduced:

$$< d_j >= d_0 b_d^j, < L_j >= L_0 b_L^j \qquad (9)$$

$$< d_j^R >= \frac{2 < d_j >}{1+\xi}, < L_j^R >= \frac{2 < L_j >}{1+\zeta}, < d_j^L >= \xi < d_j^R >, < L_j^L >= \zeta < L_j^R > \qquad (10)$$

where ξ, ζ – coefficients of branching asymmetry, indexes R,L denote the daughter vessel on the right and left downstream, respectively, $< a >= (a^L + a^R)/2$ – average value . For the optimal systems $\gamma = 3$, $b_R = 2^{-1/3}$ [12]. For other coefficients in (9)–(10) the assumptions $b_L = b_R$, $\xi = \zeta$ are often used because of allometric scaling of the vascular beds [9,11,12]. The relations (8)–(10) can be presented in a different way $K = (1+\xi^2)/(1+\xi^\gamma)^{1/\gamma}$, where $K = ((d^L)^2 + (d^R)^2)/d_0^2$ – branching coefficient. For the most mammal circulatory beds $K = 1.1 - 1.3$ [11].

Each element in the branching arterial tree, thus, possesses the characteristic impedance $Y_j = \pi d_j^2 \sqrt{d_j/(\rho h_j E_j)}$. The system $Y_n + Y_t$ of two last elements in each branching can be considered as a new terminus for every tube with branching order $j = n - 1$ with the admittance $Y_n^/$ defined by (7). By this way we can obtain a new arterial tree with $n - 1$ branching orders terminated by $Y_n^/$ instead $Y_n + Y_t$. It is worth noting that the admittances $Y_j^/$ are quite different even for the same values of Y_t in each Windkessel element because of the tree asymmetry. By means of repeating this procedure a simple system consisting of the largest tube $(i = 0)$ terminated by the effective terminus Y° can be finally obtained. The geometrical and mechanical

properties of the whole arterial bed will be, thus, included in Y°. The initial vascular tree and the system $Y_0 + Y^\circ$ will exhibit the same abilities in wave reflection.

The simplest case of the symmetrical branching tree with $K = 1/2$, $\gamma = 3$ and unrealistic relation for the lengths $L_j = L_0/(j+1)$ was investigated earlier [8]. In the present work the influence of parameters ξ, ζ, b_R, b_L on the pulse wave reflections and on the resonant properties of different asymmetrical vascular beds was investigated numerically.

Results and discussion

The experimental data shows that $h_j = \lambda d_j$, $\lambda = 0.14 - 0.2$, $E = (6-9)*10^5$ Pa and $E = (1-2)*10^6$ P for the arteries of elastic and muscle types, respectively [1]. For the geometrical parameters in (8)–(10) the following values corresponding the structure of the vascular beds of inner organs were used: $\xi, \zeta = 0.2 \div 1$, $K = 1.0 \div 1.3$, $b_L, b_R = 0.6 \div 0.9$ [11,13]. Only self-similar trees were considered in terms of independency of the geometrical parameters $\xi, \zeta, K, b_{L,R}$ from the branching order i. The scatter of distances from the input section of the largest artery to the places of wave reflection is monotonically increases with the $\xi, \zeta, b_{L,R}$ decreasing. For more symmetrical trees this scatter is relatively small and the trees will exhibit acute resonant properties because of quite equal times of the backward pulse waves traveling from different bifurcations with the same branching orders. This means that the results for asymmetric trees are more realistic. A random scattering of $< L_j >$ and $< R_j >$ values was introduced in [8] for the same reason.

The example in fig.2. shows the dependences between the dimensionless total effective admittance $Y^*(f)$ and the frequency $f = \omega/(2\pi)$ of the pulse wave at $\xi = 0.2 \div 1$. The effective admittance $Y_0^/ = Y^* Y_0$ corresponds to the system $Y_0 + Y^\circ$ and its value calculated by substituting $Y = Y_0$, $Y_t = Y^\circ$ in (7). The first maximum in $Y^*(f)$ defines the main resonant

frequency in terms [2–7]. At wide variation of ξ the main frequency variations do not exceed ± 6 Hz (at $\zeta = 0.2 \div 1$, $b_L, b_R = 0.6 \div 0.9$) and lay within the same harmonic. For the pulse rate 60–75 1/min (the frequency of the main harmonic of the pulse wave $f_0 = 1 - 1.25$) the case in fig.3 corresponds to the resonance at the 5-th harmonic. In this case the modulus of impedance is maximum at the 5-th harmonic and, thus, the correspondent component of blood flow will enter in the vascular bed of the organ. Controversially, the modulus of impedance is minimum at the 3-rd ($f = 4 - 7$ Hz) harmonic and so this component will be mostly reflected by the tree. A corresponding enhancement of the 3-rd and weakening of the 5-th harmonics can be measured on any peripheral artery out-of the vascular tree of the organ.

The findings of our calculations have shown that the influence of asymmetry in the average lengths of the arteries ζ is negligible. All the changes are observed within the same harmonic and corresponding variations do not exceed ± 2 Hz. The corresponding illustration is given in fig.4. The first relative maximum corresponds to the 5-th harmonic ($f = 15 - 18$ Hz); the first global maximum – at the 6-th harmonic ($f = 39 - 42$ Hz); the first local minimum – at the 4-th harmonic ($f = 9 - 11$ Hz). According to the terminology [2–7], $i = 5$ is the main resonant harmonic, while $i = 4,6$ are additional harmonics for the pulse diagnosis. The set of harmonics is the same for cases in fig.3–4 and depends on the L_0 only. This result matches the experimental observations [7].

The values of b_L connect not with the pathological state of the organ but with the construction peculiarities of its arterial network because of the longitudinal tethering of the vessels to outer tissues. The variations of b_R reflect the vessel wall pathology (atherosclerosis, hypertrophy) and the pathological state of the organ (inhomogeneous blood distribution within the organ, blood outflow difficulties). Our calculations revealed that even slight variations of $\delta b_R \sim 0.1$ led to noticeable changes in the amplitudes of the resonant harmonics. Thus, the individual scattering of geometrical parameters of the bed is insignificant, whereas any

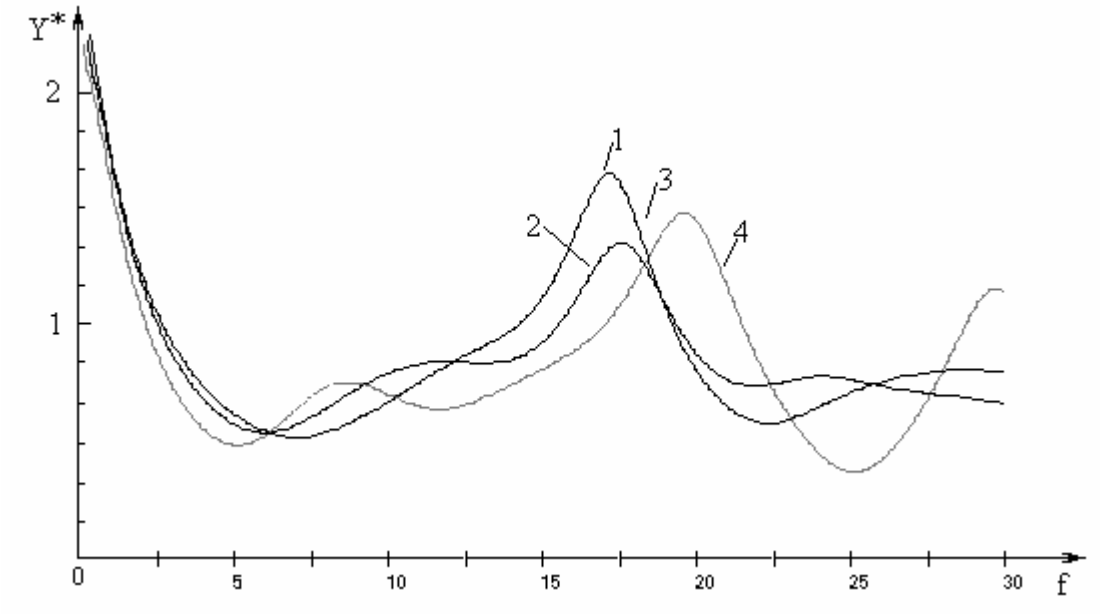

Fig.3. The dependence $Y^*(f)$ at $\zeta, b_{L,R} = 1$, $L_0 = 0.2$ m, $d_0 = 0.03$ m. The numbers 1–4 correspond to $\xi = 0.2;0.4;0.6;0.8$ respectively.

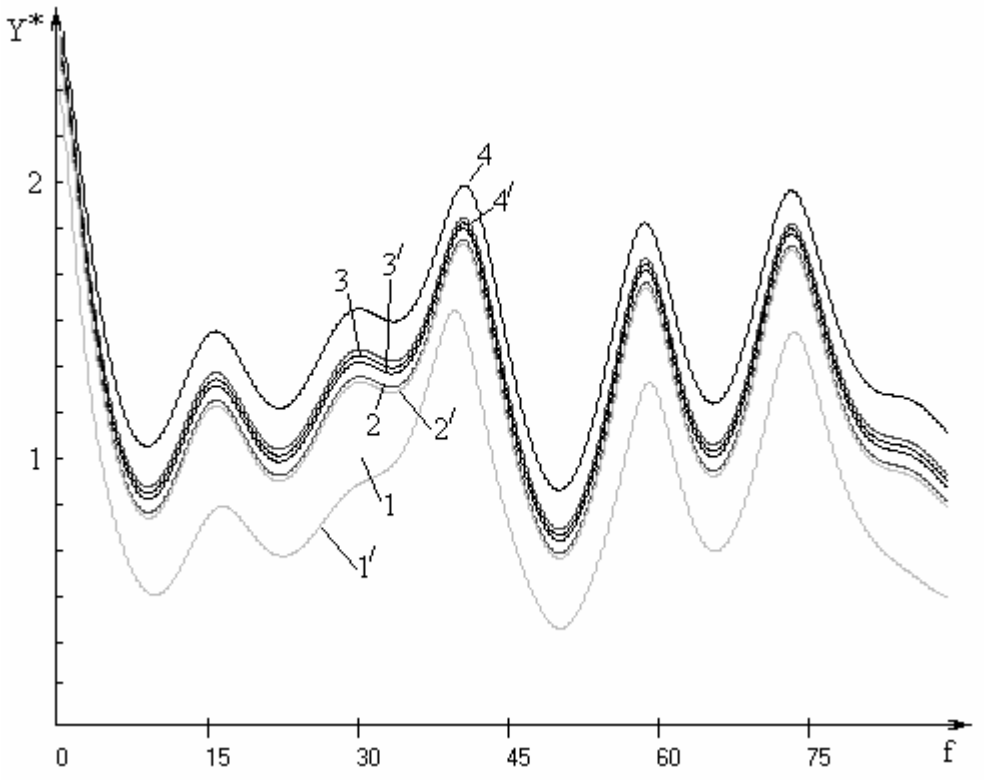

Fig.4. The dependence $Y^*(f)$ at $\xi, b_R = 1, L_0 = 0.2$ m, $d_0 = 0.03$ m. The numbers 1–4 and $1^{/} - 4^{/}$ correspond to $\xi = 0.2;0.4;0.6;0.8$, $b_L = 0.6;1$ respectively.

pathological variations caused considerable alterations of the amplitudes corresponding to the resonant harmonics of the effective admittance $Y^*(f)$.

The input admittance Y^* is mostly influenced by reflection coefficient Γ_n at the terminus. The real and image parts of the admittance of the terminus $Re(Y_t)$, $Im(Y_t)$ describe the resistive and capacitive properties of the microcirculatory (capillary) bed, respectively. If $Y_n = Y_t$, then $\Gamma_n = 0$ and pulse wave reflection at the terminus is absent (fully coordinated impedances). If $Y_t = 0$, then $\Gamma_n = 1$ (reflection at the closed end of the tube). In both cases the reflection coefficient at each junction Γ_j is a complex number. In real vascular beds the extreme cases $\Gamma_n = 0;1$ are impossible. After the capillary wall rigidity increasing and in all cases of swelling, the value $Re(Y_t)$ increases, and by this way the amplitude of the backward pulse wave increases also. The wall compliance increasing causes the increasing of $Im(Y_t)$. Thus, the increasing $Re(Y_t)$ and decreasing $Im(Y_t)$ correspond to the redundancy syndrome in the terms of oriental medicine [3–6]. Respectively, $Re(Y_t)$ decreasing and $Im(Y_t)$ increasing correspond to the insufficiency syndrome.

Some results of the calculations for the symmetric tree with $L_0 = 0.1$ m and asymmetric tree with $L_0 = 0.25$ (represented in fig.1) the dependences $Y^*(m)$ are shown in fig.5–6, respectively. The influence of the variation $Re(Y_t)$ on the Y^* is significant at several (resonant) harmonics. The set of the resonant harmonics for the tree is defined by the length of the largest vessel [2]. For the self-similar vascular beds considered here it implies the influence of the so-called caliber or scale of the bed on the set of resonant harmonics. At wide variation of pathologically significant parameters $Re(Y_t)$ and $Im(Y_t)$, the amplitude of the total effective admittance of the tree undergoes maximal variations at resonant frequencies and slightly noticeable variations at other harmonics. The dependence in fig.5 agree closely the same experimental dependence obtained for the arterial tree of kidneys. In a general case the arterial

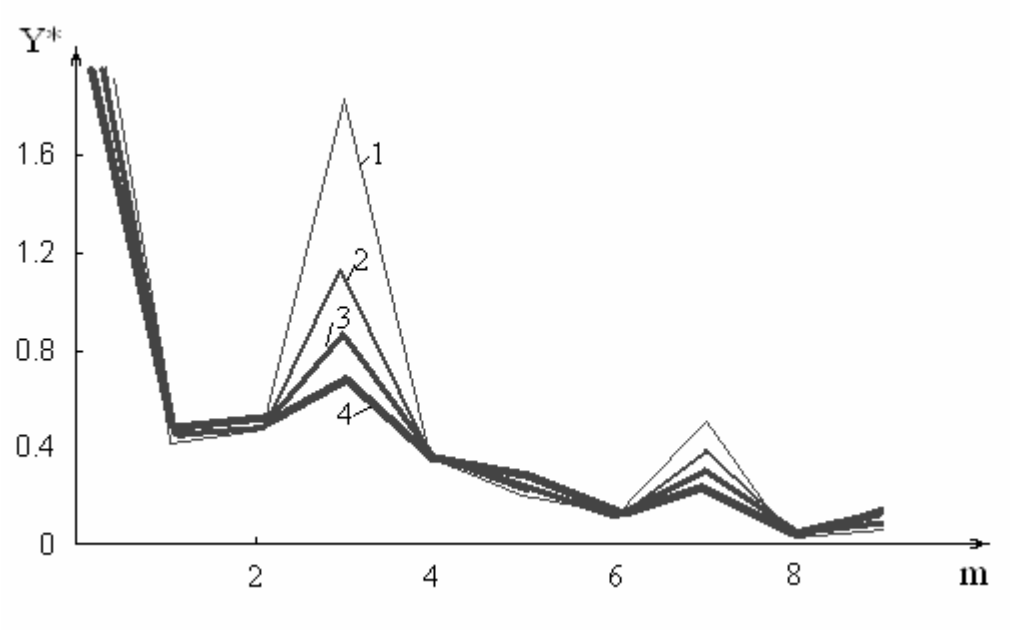

Fig.5. The dependence $Y^*(m)$ for the symmetrical arterial tree with $\xi, \zeta, b_{L,R} = 1$, $L_0 = 0.1$ m, $d_0 = 0.02$ m. The numbers 1–4 correspond to $Re(Y_t) = 0.2;0.4;0.6;0.8$ respectively.

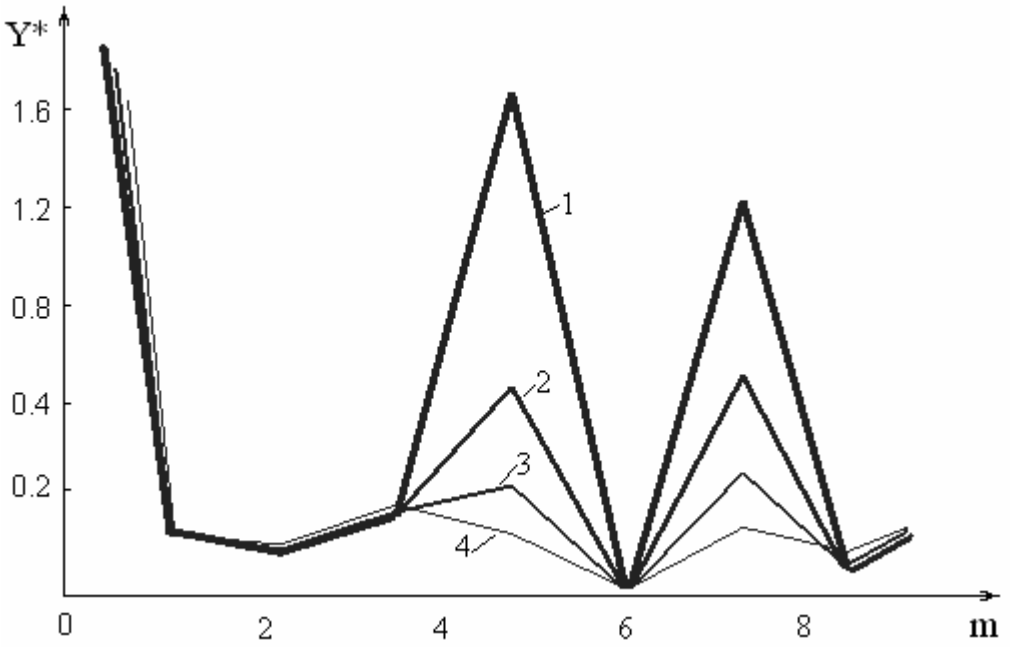

Fig.6. The dependence $Y^*(m)$ for the asymmetrical arterial tree with $\xi = \zeta = 0.7$ $b_L = 1$, $b_R = 0.9$, $L_0 = 0.25$ m, $d_0 = 0.03$ m. The numbers 1–4 correspond to $Re(Y_t) = 0.2;0.4;0.6;0.8$.

trees in kidneys are symmetrical with $b_{R,L} \sim 1$, $\xi, \zeta \sim 0.8$ [3,11]. The set of the resonant harmonics m=3;2 are the same for both dependences (theoretical, presented here and

experimental in [3]) up to the m=6, inclusively. The main resonant harmonics for $L_0 = 1-30$ cm accordingly to the calculations on the model proposed here are presented in table 1.

The proposed model should be generalized to the viscous fluid and viscoelastic longitudinally tethered tubes. In the first case all the relations (5)–(7) remain valid with $c(\omega) = c\sqrt{(1-F_w)/(1-\sigma^2)}$ instead c, where σ – Poisson's modulus for the vessel wall material, $F_w = 2J_1(z)/(zJ_0(z))$ – Womersley function, $J_{0,1}$ – Bessel's first order functions , $z = \alpha i^{3/2}$, $\alpha = R\sqrt{\omega/\mu}$ – Womersley number, $i = \sqrt{-1}$, μ – kinematical viscosity of the fluid.

Table1.

Numbers of the main and one additional resonant harmonics for different artery lengths L_0 and pulse wave velocities c.

L_0 (cm)	>25	21–25	16–21	11–16	6–11	3–6	1–3
m at $c = 5$ m/s	1;6	2;3	3;6	3;7	4;6	5;6	6;7
m at $c = 10$ m/s	2;7	3;6	4;7	4;7	5;8	6;7	7;9
m at $c = 15$ m/s	3;8	4;4	4;7	5;8	5;9	6;9	7;9
m at $c = 20$ m/s	3;8	4;5	5;8	6;9	6;5	7;9	8;10

Conclusions

1. The main features of pulse wave propagation and reflection in the arterial network of the inner organs can be investigated on the basis of the model of asymmetrically branching tree consisting of elastic tubes. The simple iterative procedure allows calculation of the total effective admittance Y^* of the system as a function of the wave frequency ω.

2. Any individual variations in geometry of a vascular bed (asymmetry of the lengths ζ and diameters ξ of the consecutive vessels, scaling parameter b_L) cause negligibly small alterations in the dependence $Y^*(\omega)$. This result provides explanation of the possibility of the pulse diagnosis of pathological state of the inner organs without preliminary knowledge of the individual vascular tree structure.
3. Any variations in pathologically significant parameters (deviations in diameters of the consecutive vessels b_R, parameters of microcirculatory bed state $Re(Y_t)$, $Im(Y_t)$) cause considerable alterations of the amplitudes of several (resonant) Fourier harmonics of the total effective admittance $Y^*(\omega)$ and slightly noticeable alterations of the amplitudes of other harmonics. The resonant harmonics correspond to the first local maximum and minimum of the function $Y^*(\omega)$ and to its global extremums, as well.
4. A set of the resonant harmonics is unique for the given arterial tree and is defined by the lengths of the vessels only. For the self-similar tree it means the dependence of the set on the length of the largest (supplying) artery of the vascular bed only, and thus on the caliber (scale) of the inner organ itself.
5. The obtained results allow to substantiate theoretically the recently proposed new pulse diagnosis method [2–7].

References

1. MILNOR W.R. Hemodynamics. Baltimore:Williams &Wilkins, 1989. 419 p.
2. WANG Y.Y., CHANG S.L., WU Y.E., HSU T.L., WANG W.K. Resonance. The missing phenomenon in hemodynamics. **Circ.Res**., 69:246-249, 1991.
3. YU G.L., WANG Y.L., WANG W.K. Resonance in the kidney system of rats. **Am.J.Physiol**., 267:H1544-1548, 1994.
4. LU W.A., CHENG C.H., LIN WANG Y.Y., WANG W.K. Pulse spectrum analysis of hospital patients with possible liver problems. **Am.J.Chin.Med**., 24:315–320, 1996..
5. WANG W.K., BAU J.G., HSU T.L., WANG Y.Y. Influence of spleen meridian herbs on the harmonic spectrum of the arterial pulse. **Am J.Chin.Med**., 28:279-289, 2000.
6. WANG W.K., HSU T.L., WANG Y.Y. Liu-wei-dihuang: a study by pulse analysis. **Am.J.Chin.Med**., 26:73-82, 1998.

7. WANG Y.Y., LIA W.C., HSIU H., JAN M.Y., WANG W.K. Effect of length on the fundamental resonance frequency of arterial models having radial dilatation. **IEEE Trans. Biomed. Eng.**, 47:313-318, 2000.
8. TAYLOR M.G. The input impedance of an assembly of randomly branching elastic tubes **Biophi s.J.** 6:29-51, 1966.
9. ZAMIR M. Mechanics of blood supply to the heart: wave refection effects in a right coronary artery. **Proc.R.Soc.Lond.B**. 265:439-444, 1998.
10. MOISEEVA I.N., REGIRER S.A. Some features of pulse wave reflections in arteries. **Fluid Dynamics.** N4:134-139, 1993.
11. SHOSHENKO K.A., GOLUB A.S., BROD V.I., et al. Architectonics of the circulatory bed. Novosibirsk, Nauka, 1982.
12. KIZILOVA N.N. The principles of organisation of transport systems in plants and animals //Proc. Conf. devoted to the 90th anniv. of A.A.Lyapunov. Novosibirsk, 2001.
13. ZAMIR M. Arterial branching within the confines of fractal L-system formalism. J.Gen.Physiol. 118:267-275, 2001.